AD-A066 153 INDIANA UNIV AT BLOOMINGTON DEPT OF CHEMISTRY F/G 7/4
MEASUREMENT AND COMPARISON OF RELATIVE FREE-ATOM FRACTIONS IN T--ETC(U)
MAR 79 K A SATURDAY, G M HIEFTJE N00014-76-C-0838
UNCLASSIFIED TR-22 NL

| OF |
ADA
066153

END
DATE FILMED
5-79
DDC

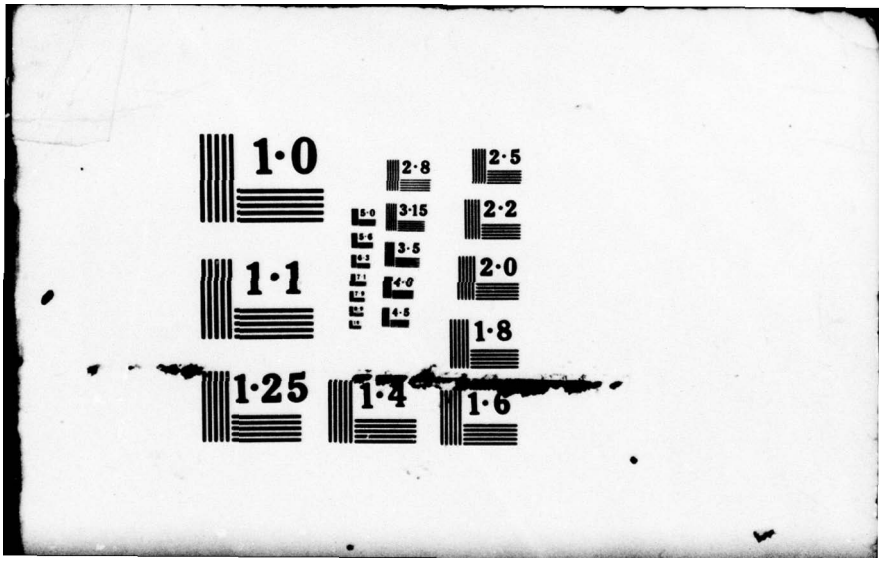
1·0
1·1
1·25
2·8
3·15
3·5
4·0
4·5
2·5
2·2
2·0
1·8
1·4
1·6

Unclassified

SECURITY CLASSIFICATION OF THIS PAGE (When Data Entered)

LEVEL II

(12)

AD A066153

DDC FILE COPY

REPORT DOCUMENTATION PAGE

READ INSTRUCTIONS BEFORE COMPLETING FORM

1. REPORT NUMBER: Seventeen	2. GOVT ACCESSION NO.
3. RECIPIENT'S CATALOG NUMBER: (9)	
4. TITLE (and Subtitle): (6) Measurement and Comparison of Relative Free-Atom Fractions in the Helium-Oxygen-Acetylene and Air-Acetylene Flames,	5. TYPE OF REPORT & PERIOD COVERED: Interim Technical Report,
	6. PERFORMING ORG. REPORT NUMBER: 22
7. AUTHOR(s): (10) K. A. Saturday and G. M. Hieftje	8. CONTRACT OR GRANT NUMBER(s): ~~N00014-76-C0838~~ N14-76-C0838 N00014-76-C-0838
9. PERFORMING ORGANIZATION NAME AND ADDRESS: Department of Chemistry, Indiana University, Bloomington, IN 47405 (11) 1 Mar 79	10. PROGRAM ELEMENT, PROJECT, TASK AREA & WORK UNIT NUMBERS: NR 051-622
11. CONTROLLING OFFICE NAME AND ADDRESS: (14) TR-22, 17	12. REPORT DATE: March 1, 1979
	13. NUMBER OF PAGES: 51
14. MONITORING AGENCY NAME & ADDRESS (if different from Controlling Office): Office of Naval Research, Washington, D. C.	15. SECURITY CLASS. (of this report): Unclassified
	15a. DECLASSIFICATION/DOWNGRADING SCHEDULE

16. DISTRIBUTION STATEMENT (of this Report)

Approved for public release; distribution unlimited

(15) N00014-76-C-0838 (12) 54 p.

17. DISTRIBUTION STATEMENT (of the abstract entered in Block 20, if different from Report)

Prepared for publication in ANALYTICAL CHEMISTRY

DDC RECEIVED MAR 22 1979 D

18. SUPPLEMENTARY NOTES

19. KEY WORDS (Continue on reverse side if necessary and identify by block number)

Flame spectrometry, atomic absorption, atomic fluorescence, atomic emission, free atom fraction, atomization efficiency

20. ABSTRACT (Continue on reverse side if necessary and identify by block number)

The determination of free atom fractions for Cu, Fe, Cr, Ca, Sr, and Ba in the helium-oxygen-acetylene and air-acetylene flames reveals the enhanced atom formation environment of the helium-diluted flame. Values ranged from unity for Cu in both flames to 0.0089 and 0.0035 for Ba in the helium-oxygen-acetylene and air-acetylene flames, respectively. Comparison of the results obtained from this study with literature values places the atom formation capabilities of the helium-diluted flame intermediate between those of the air-acetylene and nitrous oxide-acetylene flames. However, unlike the

DD FORM 1 JAN 73 1473 EDITION OF 1 NOV 65 IS OBSOLETE S/N 0102-014-6601 | Unclassified SECURITY CLASSIFICATION OF THIS PAGE (When Data Entered)

176 685 79 03 19 077

20. continued

nitrous oxide-acetylene flame, the helium-oxygen-acetylene flame has a low intensity, relatively unstructured background emission spectrum similar to that of the air-acetylene flame. In this study, a complete examination of the flame temperature, width, and sample introduction efficiency was performed for both flames in order to employ the relative integrated absorption technique for the measurement of free atom fractions. A new capillary burner, adapted to a commercial nebulization device, was designed for the study and allowed the safe use of the helium-oxygen-acetylene flame without requiring external cooling.

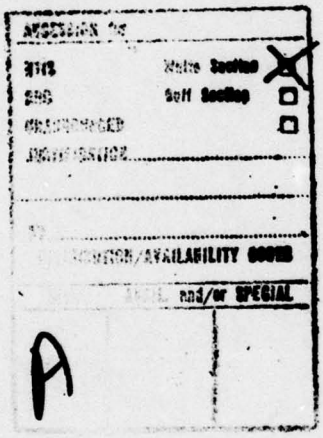

Measurement and Comparison of Relative Free-Atom Fractions in the Helium-Oxygen-Acetylene and Air-Acetylene Flames

K. A. Saturday and G. M. Hieftje*

Department of Chemistry

Indiana University

Bloomington, Indiana 47401

BRIEF

The free atom fractions for six elements in the helium-oxygen-acetylene and air-acetylene flames were measured and show the helium-diluted flame to be intermediate in atom formation capabilities between the air-acetylene and nitrous oxide-acetylene flames.

ABSTRACT

The determination of free atom fractions for Cu, Fe, Cr, Ca, Sr, and Ba in the helium-oxygen-acetylene and air-acetylene flames reveals the enhanced atom formation environment of the helium-diluted flame. Values ranged from unity for Cu in both flames to 0.0089 and 0.0035 for Ba in the helium-oxygen-acetylene and air-acetylene flames, respectively. Comparison of the results obtained from this study with literature values places the atom formation capabilities of the helium-diluted flame intermediate between those of the air-acetylene and nitrous oxide-acetylene flames. However, unlike the nitrous oxide-acetylene flame, the helium-oxygen-acetylene flame has a low intensity, relatively unstructured background emission spectrum similar to that of the air-acetylene flame. In this study, a complete examination of the flame temperature, width, and sample introduction efficiency was performed for both flames in order to employ the relative integrated absorption technique for the measurement of free atom fractions. A new capillary burner, adapted to a commercial nebulization device, was designed for the study and allowed the safe use of the helium-oxygen-acetylene flame without requiring external cooling.

Greater demands are placed on the performance of the atom cell than on any other component of an atomic spectrometric instrument. In its role as sample atomizer, an analytical flame must desolvate aerosol droplets of analyte solution, vaporize the resulting salt particles and dissociate any molecules which are formed, in order to maximize the total number of atoms available for spectroscopic detection. In addition, the flame must provide an environment which is free from physical or chemical interferences, causes minimal ionization and has a low background emission level.

Because of the importance of the flame to analytical spectroscopy, a continuing search for new flame cells exists. Although most of this search has been empirically based, and sought to employ flames which exhibited high temperatures and low burning velocities, a recent group of studies (1-5) has examined the role of the flame from a more basic viewpoint. In those studies, an isolated-droplet sample-introduction technique (1, 2) was employed to characterize the processes taking place in atom formation. In the course of those studies, it was discovered that flame gas thermal conductivity played an important role in sample atomization (3). To test that hypothesis, a helium-oxygen-acetylene flame was explored, and yielded higher emission signals than an air-acetylene flame of similar composition (4). In addition, the

desolvation rate of injected analyte droplets nearly doubled when helium was used in the flame gas mixture.

A recent examination of the physical characteristics of the helium-oxygen-acetylene flame has shown it to be a viable atom source for atomic spectroscopy (6). Many of the flame's undesirable characteristics, such as increased occurrence of flashback and thermal deformation of burner components, were noted upon its introduction (4). Fortunately, modifications in burner design overcame these drawbacks, and safe operating conditions for the flame were specified (6). The stabilized flame was found to possess a high degree of laminarity, similar to that found in the air-acetylene flame. Its background emission spectrum, although of greater intensity than that of an air-acetylene flame, was relatively unstructured.

To assess the analytical utility of this new flame cell, its efficiency of atom formation must be measured. One gauge of atom formation capabilities is the free atom fraction (7), which is the ratio of the number of species of a particular element present in the free atomic state to the total number of atoms injected into the flame. Although this quantity gives no indication of the mechanism or kinetics involved in the atom formation process, it does provide a reliable measure of the flame's ability to produce atoms. By determining free atom fractions, one

can obtain an analytically useful estimate for the combined results of different flame processes, including vaporization, ionization and compound formation.

In the present study, the free atom fractions for six elements were measured in both the air-acetylene and helium-oxygen-acetylene flames, in order to provide a basis for comparison. Other studies have determined the free atom fractions for various elements in several conventional analytical flames (8-14), including the air-acetylene flame (9-14). Unfortunately, the evaluation of a new flame-gas mixture using the results of these former studies is difficult, because a range of values has been reported for the free atom fraction of any specific element in a particular flame gas mixture. The disparity in these results arises from the differences in experimental conditions and instrumentation used by the various researchers. For this reason, identical experimental methods and equipment have been used here in the determination of free atom fractions in both the air-acetylene and helium-oxygen-acetylene flames.

In addition to the absorption measurements that are required to measure free atom fractions using the integrated absorption technique (8-10), differences in the flame environment that affect atom formation were quantified. Studies of flame temperatures, nebulization efficiencies and flame width have been per-

formed to account for the different environments. A computer-assisted data acquisition system for the measurement of the integrated absorption was designed for this work, and a capillary burner was constructed which allows a commercial nebulization device to be used with the helium-oxygen-acetylene flame.

In these investigations, the free atom fractions for Cu, Fe, Cr, Ca, Sr, Ba were found to be 1.04, 0.97, 0.41, 0.22, 0.20, and 0.0089, respectively, in the helium-oxygen-acetylene flame, and 1.00, 0.51, 0.22, 0.079, 0.090, and 0.0035, respectively, in the air-acetylene flame. The nebulization efficiency for the helium-diluted flame was 9.9% at an uptake rate of 2.0 mL min^{-1}, compared to 16.5% for the air-acetylene flame. The maximum flame temperatures found for the two flames were 2525 K in the air-supported flame and 2812 K in the helium-sustained flame.

EXPERIMENTAL

Equipment.

Burner. The burner employed in this study is a slightly modified version of a previously described capillary burner which utilized a bundle of hypodermic tubing to form a burner head (15). Sections of stainless steel hypodermic needles (Popper and Sons, Inc., New Hyde Park, N.Y.), approximately thirteen centimeters in length, were joined using high-temperature epoxy (Eccobond 104,

Emerson and Cuming, Inc., Canton, Mass.) and treated according to manufacturer's directions to set the epoxy for high temperature use. The resultant burner head could then be inserted into an adapter which allows the burner to be used with any of several commercially available nebulization assemblies.

For the helium-diluted flame, 181 exit ports were fabricated from 22-gauge syringe needles (0.5 mm i.d.) and packed into the burner head assembly. A similar burner head constructed from 18-gauge needles (0.8 mm i.d.) contained 60 exit ports and was used for an air-acetylene flame. Previous studies (4, 6) discussed the problem of burner deformation when the helium-oxygen-acetylene flame was employed. Water cooling was found to prevent this problem (6), when a Meker-type burner was used. With the new capillary burner head, no deformation problems were experienced and burner cooling was found to be unnecessary. For the helium-oxygen-acetylene flame, the highest operating temperature at the burner head (320 K) was attained with a fuel-lean mixture. For the air/acetylene flame, an operating temperature of 370 K was reached regardless of the acetylene/oxygen (fuel/oxidant) flow ratio.

Nebulizer. The capillary burner was mounted by means of an adapter onto a commercial nebulization chamber equipped with an impingement bead (Chamber: Model No. 20851-01, Nebulizer: Model No. 25958, Instrumentation Laboratories, Inc., Lexington,

Mass.). For the helium-containing flame, a constant mixture of 8.4 L min^{-1} helium and 2.4 L min^{-1} oxygen (78% He) was used as the nebulizing gas. With this constant mixture, a uniform nebulization rate ensued regardless of the fuel/oxidant flow ratio selected. For the air/acetylene flame, 10.8 L min^{-1} of air was used as the nebulizing gas flow.

All gases were supplied and mixed, when necessary, with the same type of control system described previously (6). All flows were measured using a wet-test meter (Model No. 63114, Precision Scientific Co., Chicago, Ill.) to correct for any back pressure caused by the nebulizer.

Optical System. Radiation from a 300 W integral-parabolic-reflector Eimac arc lamp (Model No. VIX-300UV, Varian Eimac Division, San Carlos, Calif.) which was operated at 15 A, was focussed into the center of the flame using a 38 mm plano-convex quartz lens (10 cm focal length). A similar lens of 8 cm focal length was used to refocus the image of the arc onto the monochromator entrance slit. An iris diaphragm (~0.4 cm) was placed directly in front of the Eimac lamp housing to act as a spatial filter and thereby eliminate from the final image a majority of light from the turbulent region of the lamp (16). A second iris, placed just before the second lens, functioned as an aperture stop for the system. Back illumination of the monochromator in-

dicated that a section of the flame approximated by a rectangle 3 mm high and 1 mm wide was observed with this optical system.

Spectrometer and Detection System. The continuum radiation was mechanically modulated at 480 Hz by a chopper placed between the light source and the first lens. After passing through the optical system, the radiation was spectrally dispersed by a 0.35 m Czerny-Turner-mount, digital step-scanning monochromator (Model EU-700, GCA/McPherson Instrument, Acton, Mass.), operated with a 0.098 mm spectral slit width and a 3 mm slit height. The radiation transmitted by the monochromator was detected by an R446 photomultiplier (Hamamatsu Corp., Middlesex, N.J.) operated at 400-600 volts (Model 244 high-voltage supply, Keithley Instruments, Inc., Cleveland, Ohio). The exact operating voltage was that required to produce a nearly full-scale response at the output of the detection system described below.

The AC current signal from the photomultiplier was converted to a proportional voltage (Model 427 Current Amplifier, Keithley Instruments, Inc., Cleveland, Ohio) and demodulated by a lock-in amplifier (Model 128, Princeton Applied Research Corp., Princeton, N.J.). The lock-in reference signal was provided by a phototransistor-lamp assembly attached to the chopper. The scale expansion feature of the lock-in was employed before the resultant signal was transferred to the data collection system or a strip-chart recorder.

Computer and Data Collection Equipment. A variable-aperture integrating analog/digital converter, VAIADC (Model 720, Keithley Instruments, Inc., Cleveland, Ohio) was used in conjunction with a PDP 12/40 computer (Digital Equipment Corp., Maynard, Mass.) to collect data for the integrated absorption measurement. Interfaces between the computer and both the VAIADC and monochromator scan controller (Model EU-700-32, GCA/McPherson Instrument, Acton, Mass.) allowed the data collection process to be synchronized with the wavelength scan. The VAIADC increased the signal-to-noise ratio of the data and allowed digital signals to be transferred to the computer (17).

The data collection program was actuated by an operator-issued command following the initial set-up of the flame-nebulizer system and electronics. A signal from the monochromator scan controller was used to trigger the integration of the output analog signal by means of the computer interrupt network. As the monochromator scanned across an absorption line, the signal was integrated for one second at each of the 0.01 mm wavelength increments. The digitized signal was retained in the computer and displayed upon a monitor for operator evaluation. Records of the digitized data were compactly stored on magnetic tape. Further details about the program and interfaces are available elsewhere (18).

Determination of Free Atom Fraction.

The free atom fraction, β, has been defined as the ratio of the number of free atoms of a particular element to the total number of atoms of that element present in the flame as ions, molecules, or free atoms (19). Consequently, the determination of β-factors requires both a measurement of the efficiency of total sample introduction into the flame and a determination of the number of free atoms in the flame. The latter quantity can be found through careful spectroscopic measurements.

In the present study, the method used to determine free atom fractions is based on the method of de Galan and Winefordner (11). In this method, the free atom fractions are calculated from the fraction of continuum source radiation absorbed by the atoms in the flame. Extending their equation (11) to include non-resonance transitions, the free atom fraction is given by:

$$\beta = \left(\frac{mc^2}{\pi e^2}\right)\left(\frac{B(T_F)}{\lambda^2 g f}\, e^{E/kT_F}\right)\left[\frac{sT_F(1345 \epsilon V_{LIQ} + V_{GAS}\, n_F/n_R)}{T_R L \epsilon \gamma V_{LIQ}}\right]\left(\frac{\alpha}{c}\right) \quad (1)$$

where m and e are the mass and charge of the electron; $B(T_F)$ is the electronic partition function for the element of interest at T_F, the flame temperature; λ and f are the wavelength and oscilla-

tor strength of the transition being employed; g and E are the statistical weight and energy of the lower level of the transition; T_R, the room temperature; s, the spectral bandpass of the monochromator; L, the path length through the flame; γ, the efficiency of desolvation of aerosol droplets in the flame; ϵ, the nebulization efficiency; V_{LIQ}, the uptake rate of the nebulizer; V_{GAS}, the flow rate of flame gases; α, the fraction of continuum radiation absorbed by atoms in the flame; C, the concentration of analyte in the solution; c, the velocity of light; k, the Boltzmann constant; and n_F/n_R, the molar ratio of burnt to unburnt flame gases. In equation (1), the first factor is composed of physical constants, whereas the second factor consists primarily of constants dependent on the element and transition being studied. The third factor contains terms which are governed by the nebulizer, flame gas mixture and observation height in the flame. The terms of the final factor are dependent on the particular solution concentration selected.

Several assumptions are made in the derivation of equation (1) which define the experimental conditions which must be used. First, equation (1) requires that light absorbed by the flame, α, be only a few percent of the total incident continuum radiation. The spectral bandpass of the monochromator, s, must be several times larger than the absorption line width, but still allow a measurable absorbance to be obtained (11). The production of a uniform atom

population throughout the flame is also assumed (10). In addition, accurate values for the oscillator strengths must be known and the selected concentrations of analyte must yield absorbances which lie on the low-optical-density portion of the absorption growth curve.

The determination of relative free atom fractions was introduced (8) and utilized in several studies (8-10) to circumvent the problems arising from the use of equation (1) to calculate absolute quantities. In the calculation of absolute free atom fractions, a correction factor must be applied to the results of equation (1) to account for the nonuniformity of the atom distribution in the flame. With the relative method, the value of equation (1) for the element of interest is ratioed with the value obtained for a reference element. Ordinarily, this reference element has a known free atom fraction of unity. The determination of the magnitude of the correction for nonuniformity is thereby circumvented with the relative technique. Also, the first factor in equation (1) need not then be evaluated, because these quantities cancel during the ratioing procedure.

The values of the system constants required for the evaluation of equation (1) are given in Table 1. The molar ratio of burnt to unburnt gases, n_F/n_R, was evaluated according to the method of Gaydon and Wolfhard (20), assuming the flame tempera-

tures which are given. The spectral bandpass, s, was determined from the width at half-intensity of a wavelength scan over a hollow cathode line. As required, the spectral bandpass far exceeds the absorption linewidth. The electronic partition functions were calculated from data tabulated by de Galan, Smith and Winefordner (21) for each of the elements. Although no experimental evidence exists for the extent of desolvation in the flame, γ, the value was assumed to be unity (22).

Measurement of Integrated Absorption. Because equation (1) is restricted to atom concentrations in the linear portion of the absorption growth curve, a preliminary experiment was performed to determine the optimal solution concentration range for each element. In addition, the observation height giving greatest integrated absorbance was ascertained. For each of the elements studied, a series of dilutions was made from stock solutions prepared by a standard method (23); these solutions were employed in the construction of an absorption growth curve. From this curve, a range of solution concentrations was selected from the low optical density region for use in the free atom fraction determination. An absorbance versus height profile was constructed for one solution concentration to determine the region of maximum absorbance for each element in each of the flame gas mixtures.

The α/C ratio, which is constant for a particular element, was evaluated by averaging the values obtained for several solu-

tion concentrations in the optimal concentration range. Multiple measurements of the α values for each solution concentration were made at the selected observation height in the flame. To determine the fraction of continuum radiation absorbed, α, numerical integration techniques were applied to the digitized wavelength-scan data that were stored on magnetic tape (see section above and Ref. 18 for further details). Values for α as low as 0.6% could be measured with this system. A precision of ±10% could be obtained in the resulting α values, giving comparable precision to that found in other studies (8, 12).

Determination of Sample Introduction Efficiency. The sample introduction efficiency, ϵ, is defined as that fraction of the total volume of aspirated solution which reaches the flame (24). To determine ϵ, 10 mL of a 100 μg mL^{-1} manganese solution was introduced into the flame at a constant rate of 2 mL min^{-1} with either the helium-oxygen mixture or air acting as the nebulization gas. The condensed manganese solution was collected from the nebulizer drain tube and was rinsed from the walls of the burner and spray chamber. After dilution to 100 mL, the concentration of the resulting solution was determined by atomic absorption. By difference, the amount of analyte reaching the flame and the sample introduction efficiency could be computed.

Determination of Flame Temperature. The flame temperature both appears directly in the free atom fraction equation, and

must also be known to calculate the electronic partition function, $B(T_F)$. Vertical temperature profiles were measured in the center of the flame using the sodium line-reversal technique (25, 26). A ribbon-filament tungsten lamp (No. 18A/T10/2P, General Electric Co., Cleveland, Ohio) with a variable-current supply was used to produce the reversed condition, which was detected by use of a wavelength modulated monochromator and synchronous detection system (27). An optical pyrometer (Pyrometer Instrument Co., Northvale, N.J.) was employed to determine the filament temperature. A tungsten-filament strip lamp with a temperature certification traceable to the National Bureau of Standards was used to periodically check the pyrometer's calibration.

Flame Width Measurements. Because of expansion of the flame gas mixture upon combustion, the path length through the flame, L, cannot be considered to be equal to the burner dimensions, or to be constant with flame height. To measure flame width, a 100 $\mu g\ mL^{-1}$ sodium solution was aspirated into both the helium-oxygen-acetylene and air-acetylene flames. The emission from the sodium in the flame provided a visible reference for the edges of the flame. From the projected images of photographic slides taken of a calibrated scale and either the air-acetylene or helium-oxygen-acetylene flame at various fuel/oxidant flow ratios, the flame width could be easily measured as

a function of height in the flame. Previous studies have measured appreciable sodium concentration near the flame boundaries (10), lending credence to this method.

RESULTS AND DISCUSSION

In this section, evaluation of parameters necessary for calculation of the free atom fraction will first be discussed, after which the significance of the free atom fractions will be considered.

Sample Introduction Efficiency. Because the driving force for the creation of a spray is related to the density of the nebulizing gas (28), the helium-oxygen mixture is a less efficient nebulization gas than air. Table 2 lists the sample introduction efficiency for both the helium-oxygen-acetylene and air-acetylene flames. For both flames, the oxidant gas mixture provided the force for nebulization and was held constant at 10.8 L min^{-1}. The sample uptake rate was also held constant at 2 mL min^{-1}.

As expected, the sample introduction efficiency is lower for the helium-containing mixture and was found to be 60% that of the equivalent air-acetylene flame. Of course, the amount of sample reaching either flame per unit time could be increased by raising the sample uptake rate, but the efficiency would then be

expected to decrease (29). For example, Table 2 reveals the small increase in sample delivery rate to the flame which is caused by doubling the nebulizer uptake rate in the helium-oxygen-acetylene flame. In further work, the lower uptake rate (2 mL min^{-1}) was chosen for the determination of free atom fractions because it yielded greater flame stability.

Flame Temperature Measurement. Figures 1 and 2 display vertical temperature profiles in the helium-oxygen-acetylene and air-acetylene flames at different values of the fuel/oxidant, F/O, flow ratio. The precision of the measurements in both flames was ±1% (relative standard deviation). To check the data reliability, temperatures were determined with a series of different sodium concentrations in the flame. No temperature difference was found over the range (50-2500 μg/mL Na) of solutions tested.

In the air-acetylene flame (cf. Fig. 1), a rapid increase in temperature is observed just above the primary reaction zone. The increase is greatest for the fuel-lean flame (Curve D, Figure 1), where a 100 K increase occurs in the region one centimeter above the primary reaction zone (0.0 cm on the plot). Other investigators have observed similar increases (100 K in fuel-lean flames and 30 K in fuel-rich flames) and have attributed them to the establishment of dissociation equilibrium among the flame species (30, 31). In this region, flame species which are formed in excess of their equilibrium concentration in the reaction zone

recombine exothermically until an equilibrium is reached.

In the helium-oxygen-acetylene flame, no significant temperature increase is observed above the primary reaction zone. As shown in Figure 2, the temperature remains nearly constant with height in the lower part of the flame at 2730 K and 2750 K, respectively, for the 0.80 and 0.90 fuel/oxidant flow ratio mixtures. However, the most fuel-lean mixture (F/O=0.70) exhibits a steadily decreasing temperature profile, and possesses the highest temperature (2810 K) measured for the helium-diluted flame. Similar profiles have been observed in a nitrous oxide-acetylene flame (32).

The relatively uniform thermal environment found in the fuel-rich helium-containing flames is important analytically. The flame atmosphere experienced by the analyte atom population under near isothermal conditions is more homogeneous than that produced in a flame with drastic temperature gradients in the analytical viewing region. The analytical signal obtained from the atoms is more easily optimized and less dependent on small variations in instrumental conditions, when uniform flame conditions are present.

The reasons for the existence of the constant-temperature region in the helium-diluted flames are the basis for some conjecture. The radical physical properties of helium undoubtedly contribute to the production of the isothermal environment, and

make the helium-oxygen-acetylene flame quite different from the air-acetylene flame. As a result of helium's high thermal conductivity, heat will be conducted throughout the burnt gases more readily. Also, unlike the air-supported flame, temperature increases caused by the generation of heat in the secondary combustion region will be dampened in the helium-oxygen-acetylene flame by the high heat capacity of helium. Instead, diffusion of heat from the flame will be increased. Through some combination of these and other possible processes, the energy evolved from recombination of flame species formed in the reaction zone and the combustion of excess fuel with atmospheric oxygen is evenly distributed throughout the lower portion of the flame. Clearly, further investigations are required to elucidate the mechanism for the production of the observed temperature profiles.

Unlike the fuel-rich mixtures, the fuel-lean helium-oxygen-acetylene flame exhibits a rapid decrease in temperature with increasing height in the flame. The highest temperature measured in this study for a helium-containing mixture (2810 K) was found near the primary reaction zone of the lean flame. This finding is consistent with previous studies (31) which have shown that flame temperatures in air-acetylene mixtures increase as the fuel/oxidant flow ratio approaches that required for stoichiometric CO_2 production (F/O=0.40). However, the increased flame tempera-

ture could also result from preheating of the flame gas mixture (33). Credence is lent to this hypothesis by the observation that the highest burner head temperature produced by any of the helium-containing flames was measured with the fuel-lean mixture. This preheating effect could also be the cause of the high temperature gradient present in this flame. The changes in flame gas radical concentrations produced by preheating can affect the composition of species in the body of the flame, and thereby cause different processes to occur in the post-reaction zone. Any variations in the processes taking place in the flame, coupled with a decreased amount of excess acetylene available for secondary combustion, could change the shape of the temperature profile. Unfortunately, the proof of these hypotheses is beyond the findings and scope of the present study.

Flame Width Measurements. In Figures 3 and 4, a large variation in flame width with fuel-oxidant ratio is observed for both flames used in the present study. The greater flame width for the helium-oxygen-acetylene flame is indicative not only of the expansion of the combustion products because of a higher temperature environment and the increased diffusion rate of helium, but also of the increased degree of dissociation which affects the molar ratio of burnt to unburnt gases.

In correlating the results of the flame width and temperature determinations observed in Figures 1-4, one notes an unexpected

decrease in flame width with increasing flame temperature. Preheating of the flame gases, which was discussed in the flame temperature section above, could be the cause of this observation also. In the burner, the flow of gases is accelerated by the warming process, causing the gases to issue from the burner port at an increased velocity. The flame produced by the preheated gases will then be longer and thinner in shape and will possess a higher burning velocity (33). The results obtained in this study indicate some preheating could be occurring in both gas mixtures.

Secondary combustion of the flame gases could also account for the increased flame width at high fuel/oxidant ratios. As the gas mixture deviates from the stoichiometric ratio, a smaller percentage of the flame gases are consumed in the primary combustion region. For the fuel-rich mixtures considered in the present study, the excess fuel is available for secondary combustion with entrained atmospheric oxygen. Obviously, this secondary combustion would be most pronounced at the flame edge, where atmospheric entrainment takes place. In turn, additional combustion at the flame boundaries would increase the effective flame width.

Relative Free Atom Fractions.

Six elements were selected for study in the helium-oxygen-

acetylene flame. These elements display a wide variation in free atom fractions in the air-acetylene flame (9-12, 14) and are dependent on flame gas composition to different extents (12). The transitions selected for this study are not always those most commonly used for routine analysis, but are those which displayed a high relative absorbance compared to other possible transitions (34). For all the transitions utilized in this study, the lower energy level was the ground state, making the exponential term of equation (1) unity. Pertinent physical parameters of the selected transitions are compiled in Table 3. For every element except copper, the listed oscillator strengths are averages of the referenced literature values. The oscillator strength value of copper was obtained from a critical review of published data on the Cu I transition (39).

The numerical value of the free atom fraction is dependent mostly on the observation position in the flame and the composition of the flame gas mixture. In most experimental systems, the gas composition can be precisely controlled, leaving the height of observation in the flame as the primary variable in the determination of free atom fractions (50). To assess the importance of viewing height in the flame on the measurement of free atom fractions, a study of atom population versus flame position was done for both the helium-oxygen-acetylene and the air-acetylene flames.

In Figure 5, the atom population at different heights in the flame is indicated by the measured value of ^{o}, the fraction of continuum radiation absorbed by the atoms per unit of flame width. The observed variation in atom population with changes in the flame environment is strongly dependent on the kind of element. The relatively flat profiles of Fe and Cu in both flames reflect the high degree of atomization for these elements, and their insensitivity to flame composition. In contrast, flame chemistry is known to affect markedly the formation of Ca, Ba, Cr and Sr atoms (12), behavior which can be readily observed in Figure 5.

The observation heights to be employed for the determination of free atom fractions were selected using Figure 5. For each element, the height corresponding to the optimal atom population in each of the four flame-gas mixtures was used for the measurement of the free atom fraction. Examination of Figure 5 indicates the deviations in evaluated free atom fractions that would occur if only one observation height were selected for all elements. For example, if the only observation height used were that optimal for Ca absorbance in the fuel-rich air-acetylene flame (i.e. 2 cm above the burner top), non-optimal values of the free atom fraction would be obtained for most other elements. As a result, the true performance of the flame could not be assessed. In this study, the best conditions for the evaluation

of the free atom fractions were sought in order to accurately appraise the performance of the flames.

A comparison of the relative free atom fraction in both fuel-rich and fuel-lean air-acetylene and helium-oxygen-acetylene flames is given in Table 4. In the calculation of these values, copper was used as a reference element and was assigned a free atom fraction of unity in the fuel-rich air-acetylene flame (9, 10). To obtain the relative free atom fractions, the values of equation (1) for all other elements were ratioed to that of copper in the fuel-rich air-supported flame.

In the two air-acetylene flame compositions examined, the relative free atom fractions for Ca, Cu, Fe and Sr remain relatively constant, while Ba and Cr exhibit large differences. The results for Fe and Cu are expected, because the atom formation characteristics of these elements are known to be rather independent of flame chemistry. On the other hand, Ca, Sr, Ba and Cr exhibit strongly environment-dependent atom production, which is evident from the atom population profiles of Figure 5. The free atom fractions of Ca and Sr are similar for the two gas mixtures, not because their atom formation processes are independent of flame composition, but because of the production of similar atom populations at the optimal but different viewing height for both flame gas mixtures.

Unlike the air-acetylene flame, the helium-oxygen-acetylene

flame produces, for all six elements, free atom fractions which vary little with flame composition. The atom population profiles are also remarkably independent of flame composition (cf. Fig. 5), despite the different temperature profiles exhibited by the two helium-diluted mixtures. These results indicate that a thermal mechanism is probably not dominant in the atom formation process in the helium-oxygen-acetylene flame, although the high thermal conductivity of helium might play an important role. Mechanisms have recently been proposed for the air-acetylene flame in which various flame species have been shown to contribute to the atom formation process (30, 51, 52). Similar mechanisms might be operative during atom production in the helium-diluted flame, but no evidence for any specific mechanism can be gleaned from the results now available.

Although no explanation for increased atom production can be substantiated, the helium-diluted flame clearly shows larger free atom fractions for all elements not ordinarily considered to be totally atomized in the air-acetylene flame. Table 4 indicates the relative (cf. "ratio" column) increases found in the helium-oxygen-acetylene flame. To compute these ratios, the larger of the two free atom fraction values obtained for each oxidizer was used. Only Cu, which exhibits a free atom fraction of unity (within experimental error) in both flames, shows no marked improvement in the helium-diluted flame. The similar behavior of

Cu in both flames argues against the production of an increased atom population in the helium-oxygen-acetylene flame because of more efficient vaporization of desolvated particles. Any postulated atom formation mechanisms in the helium-sustained flame needs to account for this similarity.

Previous workers have measured increased atom formation rates for the helium-diluted flame (4). This increased atom production capability would not be reflected in the results of this study, however, because the local equilibrium set up in a particular flame region determines the number of free atoms present, rather than the kinetics of their release.

Table 5 compares the results of this study with those of other workers. For those studies employing the relative method of free atom fraction measurement, the reference element that was employed is listed in the footnotes of the table; all other studies were performed on an absolute basis. The values selected for inclusion in Table 5 from the present study are the larger of those obtained for each oxidant mixture (cf. Table 4).

When the values obtained by different workers for the free atom fraction of an element in the air-acetylene flame are compared, the results of the present study fall within the range of values reported in the literature. However, the free atom fractions obtained during this investigation should be slightly higher than those of other studies using the relative absorption tech-

nique, because the value used here for the oscillator strength of copper was greater than that used in other studies [0.43 compared to 0.30 (10) and 0.35 (9)].

Discrepancies in the values obtained in the air-acetylene flame can also arise from variations in the experimental conditions used by different workers. As discussed earlier, the observation height selected for each study can affect the resulting value of the free atom fraction. In addition, variations in fuel/oxidant ratio, the use of separated flames, and differences in burner design can change the atom distribution in the flame and thereby affect the measured value.

Table 5 indicates the atom formation capabilities of the helium-oxygen-acetylene flame to be intermediate between those of the nitrous oxide-acetylene and air-acetylene flames. Moreover, the helium-diluted flame performs better than the hydrogen-oxygen-argon and hydrogen-nitrous oxide flame. The hydrogen-air flame appears to possess atom production abilities similar to those of the helium-oxygen-acetylene flame, but the higher temperature environment of the latter flame should produce a higher atom population when refractory sample matrices are present.

For analytical applications, the greatest potential for the helium-oxygen-acetylene flame lies in the area of atomic fluorescence spectrometry. The higher degree of atomization and expected low quenching character of this flame gas mixture should

produce an increased atomic fluorescence signal. Investigations into the utility of this flame for atomic fluorescence are now underway in this laboratory. Additional studies are also needed to assess the degree of interference present in the flame, and to measure the detection limits it produces.

ACKNOWLEDGEMENT

The authors wish to thank John Dorsett and Larry Sexton for their help and patience in the construction of the capillary burner. Also, we are grateful to Keithley Instruments, Inc., for furnishing the variable-aperture integrating analog-to-digital convertor used in this study.

LITERATURE CITED

1. G. M. Hieftje and H. V. Malmstadt, Anal. Chem., 40, 1860 (1968).

2. G. M. Hieftje and H. V. Malmstadt, Anal. Chem., 41, 1735 (1969).

3. N. C. Clampitt and G. M. Hieftje, Anal. Chem., 44, 1211 (1972).

4. N. C. Clampitt and G. M. Hieftje, Anal. Chem., 46, 382 (1974).

5. G. J. Bastiaans and G. M. Hieftje, Anal. Chem., 46, 901 (1974).

6. K. A. Saturday and G. M. Hieftje, Anal. Chem., 49, 2013 (1977).

7. J. D. Winefordner, V. Svoboda and L. J. Cline, CRC Crit. Rev. Anal. Chem., 1, 233 (1970).

8. D. S. Smyly, W. P. Townsend, P. J. Th. Zeegers and J. D. Winefordner, Spectrochim. Acta, Part B, 26, 531 (1971).

9. P. J. Th. Zeegers, W. P. Townsend, and J. D. Winefordner, Spectrochim. Acta, Part B, 24, 243 (1969).

10. J. B. Willis, Spectrochim. Acta, Part B, 25, 487 (1970).

11. L. de Galan and J. D. Winefordner, J. Quant. Spectrosc. Radiat. Transfer, 7, 251 (1967).

12. L. de Galan and G. F. Samaey, Spectrochim. Acta, Part B, 26, 177 (1970).

13. J. B. Willis, Spectrochim. Acta, Part B, 26, 177 (1971).

14. S. R. Koirtyohann and E. E. Pickett, Proc. 13th Coll. Spectrosc. Int., Ottawa, 1967, p. 270, Hilger, London (1968).

15. K. M. Aldous, R. F. Browner, R. M. Dagnall and T. S. West, Anal. Chem., 42, 939 (1970).

16. R. L. Cochran and G. M. Hieftje, Anal. Chem., 49, 2040 (1977).

17. J. W. Frazer, G. M. Hieftje, L. R. Layman and J. T. Sinnamon, Anal. Chem., 49, 1869 (1977).

18. K. A. Saturday, Ph.D. Thesis, Indiana University, 1979.

19. J. D. Winefordner and T. J. Vickers, Anal. Chem., 36, 1939 (1964).

20. A. G. Gaydon and R. G. Wolfhard, "Flames, Their Structure, Radiation and Temperature", Chapman and Hall, London, 1970.

21. L. de Galan, R. Smith and J. D. Winefordner, Spectrochim. Acta, Part B, 23, 521 (1968).

22. C. Th. J. Alkemade, "Fundamental Aspects of Decomposition, Atomization, and Excitation of the Sample in the Flame", in "Flame Emission and Atomic Absorption Spectrometry", Vol. 1, J. A. Dean and T. C. Rains, Eds., Dekker, New York, 1969, Chapter 4.

23. J. A. Dean and T. C. Rains, "Standard Solutions for Flame Spectrometry", in "Flame Emission and Atomic Absorption Spectrometry", Vol. 2, J. A. Dean and T. C. Rains, Eds., Dekker, New York, 1971, Chapter 13.

24. J. B. Willis, Spectrochim. Acta, Part A, 23, 811 (1967).

25. W. Snelleman, Ph.D. Thesis, University of Utrecht, 1965.

26. W. Snelleman and J. A. Smit, Metrologia, 4, 123 (1965).

27. G. M. Hieftje and R. J. Sydor, Appl. Spectrosc., 26, 624 (1968).

28. W. E. Meyer and W. E. Ranz, "Sprays", in "Encyclopedia of Chemical Technology", Vol. 12, R. E. Kirk and D. F. Othmer, Eds., Interscience Encyclopedia, New York, 1954, p. 703.

29. K. Szivos, L. Polos, and E. Pungor, Spectrochim. Acta, Part B, 31, 289 (1976).

30. D. J. Halls, Anal. Chim. Acta, 88, 69 (1977).

31. W. Snelleman, "The Measurement and Calculation of Flame Temperature", in "Flame Emission and Atomic Absorption Spectrometry", Vol. 1, J. A. Dean and T. C. Rains, Eds., Dekker, New York, 1969, Chapter 7.

32. J. B. Willis, J. O. Rasmuson, R. N. Kniseley, and V. A. Fassel, Spectrochim. Acta, Part B, 23, 725 (1968).

33. A. G. Gaydon, "The Spectroscopy of Flames", Chapman and Hall, London, 1974.

34. M. L. Parsons, B. W. Smith and G. E. Bentley, "Handbook of Flame Spectroscopy", Plenum, New York, 1975.

35. N. P. Penkin and L. N. Shabanova, Opt. Spectrosk., 12, 1 (1962).

36. B. V. L'vov, J. Quant. Spectrosc. Radiat. Transfer, 12, 651 (1972).

37. W. H. Parkinson, E. M. Reeves, and F. S. Tomkins, J. Phys. B., 9, 157 (1976).

38. L. N. Shabanova, Opt. Spectrosk., 15, 450 (1963).

39. A. Bielski, J. Quant. Spectrosc. Radiat. Transfer, 15, 463 (1975).

40. C. H. Corliss and W. R. Bozman, "NBS Monograph 53", U.S. Government Printing Office; Washington, D. C., 1961.

41. M. H. Davis, P. M. Routley, R. B. King, "Proc. of the National Science Foundation Conf. on Stellar Atmospheres", Indiana Univ., p. 47, 1954.

42. G. M. Lawrence, J. K. Link, and R. B. King, Astrophys. J., 141, 293 (1965).

43. H. Buck, B. Budick, R. J. Gosher and S. Marcus, Phys. Rev., 144, 96 (1966).

44. C. W. Allen, "Astrophysical Quantities", Athlone, London, 1963.

45. C. H. Corliss and B. Warner, J. Res. Nat. Bur. Standards, 70A, 325 (1966).

46. C. H. Corliss and J. L. Tech., J. Res. Nat. Bur. Standards, 71A, 567 (1967).

47. F. P. Banfield and M. C. E. Huber, Astrophys. J., Part 1, 186, 335 (1973).

48. V. K. Prokof'ev, Z. Physik, 50, 701 (1928).

49. Y. I. Ostrovskii, N. P. Penkin and L. N. Shabanova, Sov. Phys.-Dokl., 3, 538 (1958).

50. V. A. Fassel, J. O. Rasmuson, R. N. Kniseley and T. G. Cowley, Spectrochim. Acta, Part B, 25, 559 (1970).

51. D. J. Halls, Spectrochim. Acta, Part B, 32, 221 (1977).

52. D. J. Halls, Spectrochim. Acta, Part B, 32, 397 (1977).

53. E. Hinnov and H. Kohn, J. Opt. Soc. Amer., 47, 156 (1957).

Table 1. System Constants Needed for the Determination of Free Atom Fractions

s		0.098 nm
n_T/n_R	air/acetylene	1.09 (T_F = 2500 K)
	He/O_2/acetylene	1.60 (T_F = 2750 K)
V_{GAS}	air/acetylene	
	F/O^d = 0.58	12.1 L min^{-1} (1.3 L min^{-1} C_2H_2)
	F/O^d = 0.84	12.7 L min^{-1} (1.9 L min^{-1} C_2H_2)
	He/O_2/acetylene	
	F/O = 0.70	12.5 L min^{-1} (1.7 L min^{-1} C_2H_2)
	F/O = 0.90	13.0 L min^{-1} (2.2 L min^{-1} C_2H_2)
V_{LIQ}		2.0 mL min^{-1}
T_R		298 K

s = monochromator spectral slit width

n_T/n_R = the molar ratio of burnt to unburnt flame gases

V_{GAS} = total gas flow, i.e. oxidizer plus fuel flow rate

F/O = ratio of fuel gas (C_2H_2) flow rate to oxidizer gas flow rate

V_{LIQ} = sample uptake rate of the nebulizer

T_R = laboratory temperature

T_F = flame temperature

Table 2. Comparison of Sample Introduction Efficiency[a] of the Helium-Oxygen-Acetylene and Air-Acetylene Flames

Sample Uptake[b] Rate (mL min^{-1})	Efficiency (%)		Rate of Sample Delivery to Flame (mL min^{-1})	
	$He-O_2$[c]	Air	$He-O_2$	Air
2.0	9.9 ± .3[d]	16.5 ± .5	.20 ± .01	.33 ± .01
4.0	6.6 ± .1	____	.26 ± .01	____

a. Sample introduction efficiency is the volume of sample delivered to the flame divided by the total volume of sample consumed by the nebulizer.

b. Nebulizer gas flow constant at 10.8 L min^{-1} for both $He-O_2$ and air flows.

c. Gas mixture contained 78% helium.

d. 99% confidence levels of the mean.

Table 3. Physical Constants Used in the Calculation of the Free Atom Fractions of Selected Elements

Element	Wavelength (nm)	g_i [a]	f [b]
Ba	553.5	1.0	1.46 [35-37]
Ca	422.7	1.0	1.55 [36-38]
Cu	324.7	2.0	0.43 [39]
Cr	357.9	7.0	0.24 [40-44]
Fe	248.3	9.0	0.353 [34, 45-47]
Sr	460.7	1.0	1.55 [35-36, 48-49]

a. g_i is the statistical weight of the ground state of the transition.

b. f are the average values of oscillator strengths of the transition found in the literature. The numbers in brackets are literature citations.

Table 4. Relative Free Atom Fractions[a] for the Air-Acetylene and Helium-Oxygen-Acetylene Flames

Element	air/C_2H_2		He/O_2/C_2H_2		Ratio[c]
____	F/O=0.84	F/O=0.58	F/O=0.90	F/O=0.70	He/air
Ba	.0035	.0014	.0089	.0087	2.54
Ca	.065	.079	.22	.15	2.78
Cu	1.00[a]	.86	.84	1.04	1.04
Cr	.22	____[b]	.41	.25	1.86
Fe	.46	.51	.82	.97	1.90
Sr	.080	.090	.20	.18	2.22

a. Copper was used as a reference element with an assigned free atom fraction of 1.00.

b. Absorption of Cr atoms could not be accurately measured.

c. Ratio of maximum free atom fraction in the He-O_2-C_2H_2 flame to the maximum value measured in the air-C_2H_2 flame.

Table 5. Comparison of Free Atom Fractions Present in the Helium/Oxygen/Acetylene Flame and Several Conventional Flames

Flame / Element	$He-O_2-C_2H_2$	Air - C_2H_2							$N_2O-C_2H_2$			$H_2/O_2/Ar$	H_2/N_2O	H_2/air
Ref.	This Work	This Work[a]	[9][a]	[12]	[11]	[14]	[10][a]	[53]	[10][b]	[14]	[12]	[8][c]	[12]	[12]
Ba	.0089	.0035	.0009	.0018	.0011	.0031	.0026 .0031[b]	.0021	.20	.074	.17	–	.0046	.005
Ca	.22	.079	.066	.07	.14	.052	.070 .083[b]	.0047	.94	.34	.52	-	.036	.15
Cu	1.04	1.00	1.0	.88	.98	.40	1.0 1.19[b]	.82	.68	.49	.66	.97	.92	.97
Cr	.41	.22	.065	.071	.064	.55	-	.13	-	1.00	-	-	.042	.31
Fe	.97	.51	.38	.84	.66	-	-	-	-	-	.82	-	.91	.82
Sr	.20	.090	.075	.063	.13	.068	-	.11	-	.57	.26	.094	.039	.17

a. Cu used as reference element
b. Mg used as reference element
c. Ag used as reference element

FIGURE CAPTIONS

Figure 1. Variation of temperature with height in the air-acetylene flame. Constant air flow rate, 10.8 L min^{-1}. Acetylene flow rate: A, 1.9; B, 1.7; C, 1.6; D, 1.3 L min^{-1}. Fuel/oxidant ratio: A, 0.84; B, 0.74; C, 0.68; D, 0.58. 750 µg mL^{-1} Na solution aspirated into the flame for all measurements.

Figure 2. Variation of temperature with height in the helium-oxygen-acetylene flame. Constant helium-oxygen mixture, 8.4 L min^{-1} He, 2.4 L min^{-1} O_2 (78% He). Acetylene flow rate: A, 2.2; B, 1.9; C, 1.7 L min^{-1}. Fuel/oxidant ratio: A, 0.90; B, 0.80; C, 0.70. 100 µg mL^{-1} Na solution aspirated into the flame for all measurements.

Figure 3. Variation in flame width with height in the air-acetylene flame. Constant air flow rate, 10.8 L min^{-1}. Acetylene flow rate: A, 1.9; B, 1.7; C, 1.6; D, 1.3 L min^{-1}. Fuel/oxidant ratio: A, 0.84; B, 0.74; C, 0.68; D, 0.58.

Figure 4. Variation in flame width with height in the helium-oxygen-acetylene flame. Constant helium-oxygen mixture, 8.4 L min^{-1} He, 2.4 l min^{-1} O_2 (78% He). Acetylene flow rate: A, 2.2; B, 1.9; C, 1.7 L min^{-1}. Fuel/oxidant ratio: A, 0.90; B, 0.80; C, 0.70.

Figure 5. Profiles of α, the fraction of continuum radiation absorbed, versus height in the flame.

Ca, 422.7 nm, 100 μg mL^{-1},
(a) $He/O_2/C_2H_2$ flame, (b) Air/C_2H_2 flame;

Ba, 553.5 nm, 5000 μg mL^{-1},
(c) $He/O_2/C_2H_2$ flame, (d) Air/C_2H_2 flame;

Fe, 248.3 nm, 1000 μg mL^{-1},
(e) He/O_2-C_2H_2 flame, (f) Air/C_2H_2 flame;

Cu, 324.7 nm, 50 μg mL^{-1},
(g) $He/O_2/C_2H_2$ flame, (h) Air/C_2H_2 flame;

Cr, 357.9 nm, 500 μg mL^{-1},
(i) $He/O_2/C_2H_2$ flame, (j) Air/C_2H_2 flame;

Sr, 460.7 nm, 100 μg mL^{-1},
(k) $He/O_2/C_2H_2$ flame, (l) Air/C_2H_2 flame.

○ - $He/O_2/C_2H_2$ flame (Fuel/oxidant = 0.90)
● - Air/C_2H_2 flame (Fuel/oxidant = 0.84)
□ - $He/O_2/C_2H_2$ flame (Fuel/oxidant = 0.70)
■ - Air/C_2H_2 flame (Fuel/oxidant = 0.58)

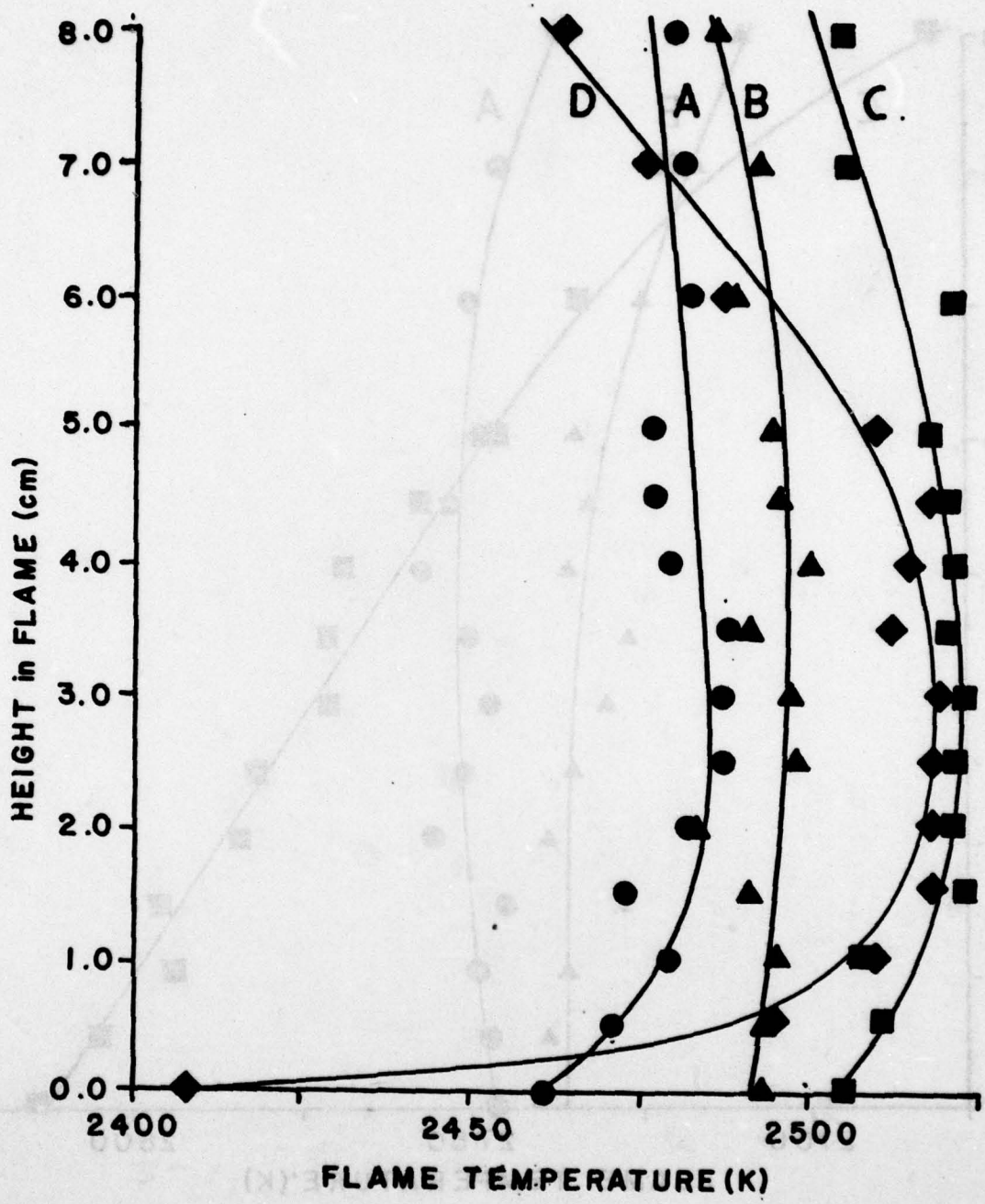
8.0
7.0
6.0
5.0
4.0
3.0
2.0
1.0
0.0
HEIGHT in FLAME (cm)
D
A
B
C
2400
2450
2500
FLAME TEMPERATURE (K)

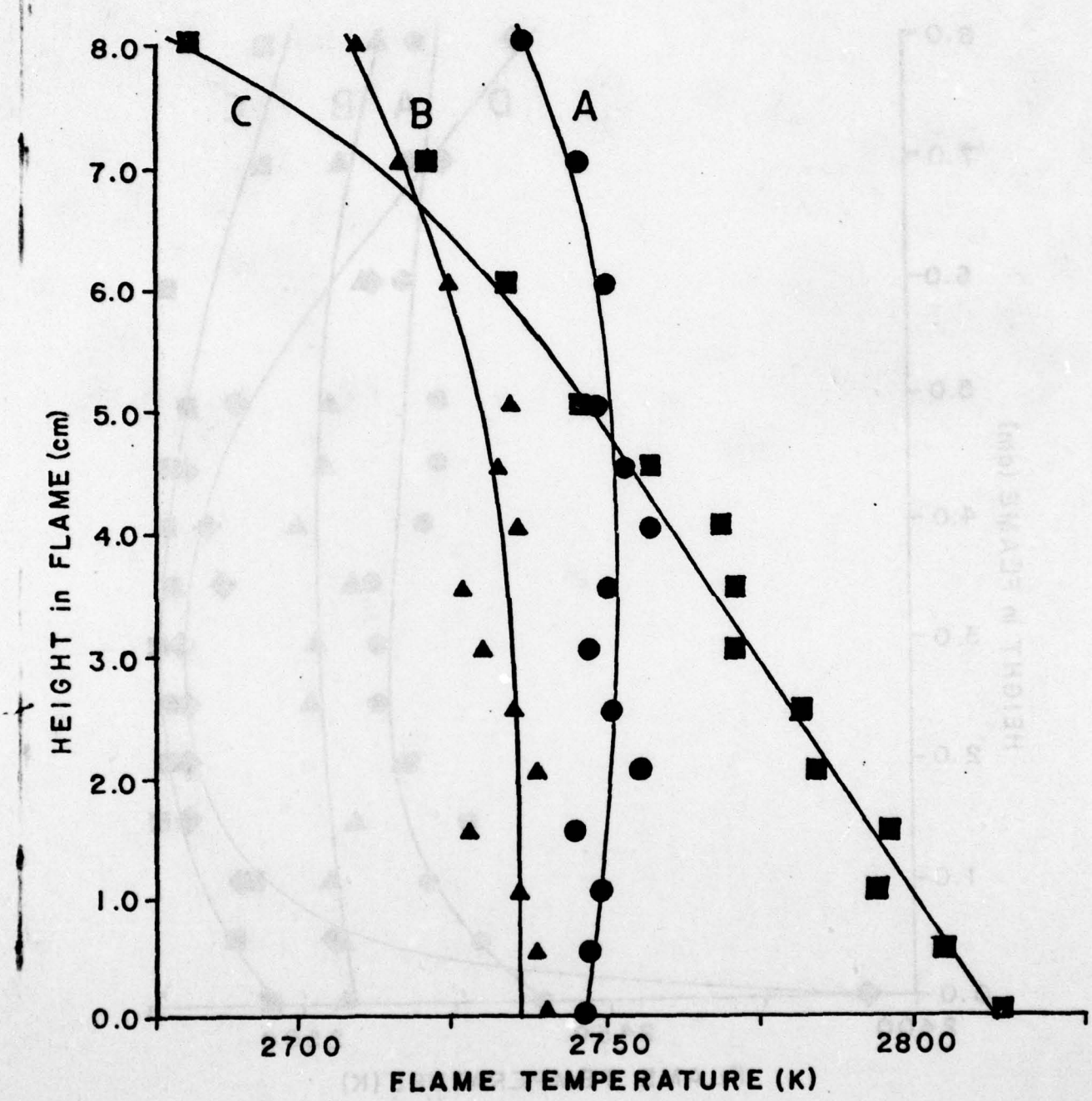
8.0
7.0
6.0
5.0
4.0
3.0
2.0
1.0
0.0
HEIGHT in FLAME (cm)
C
B
A
2700
2750
2800
FLAME TEMPERATURE (K)

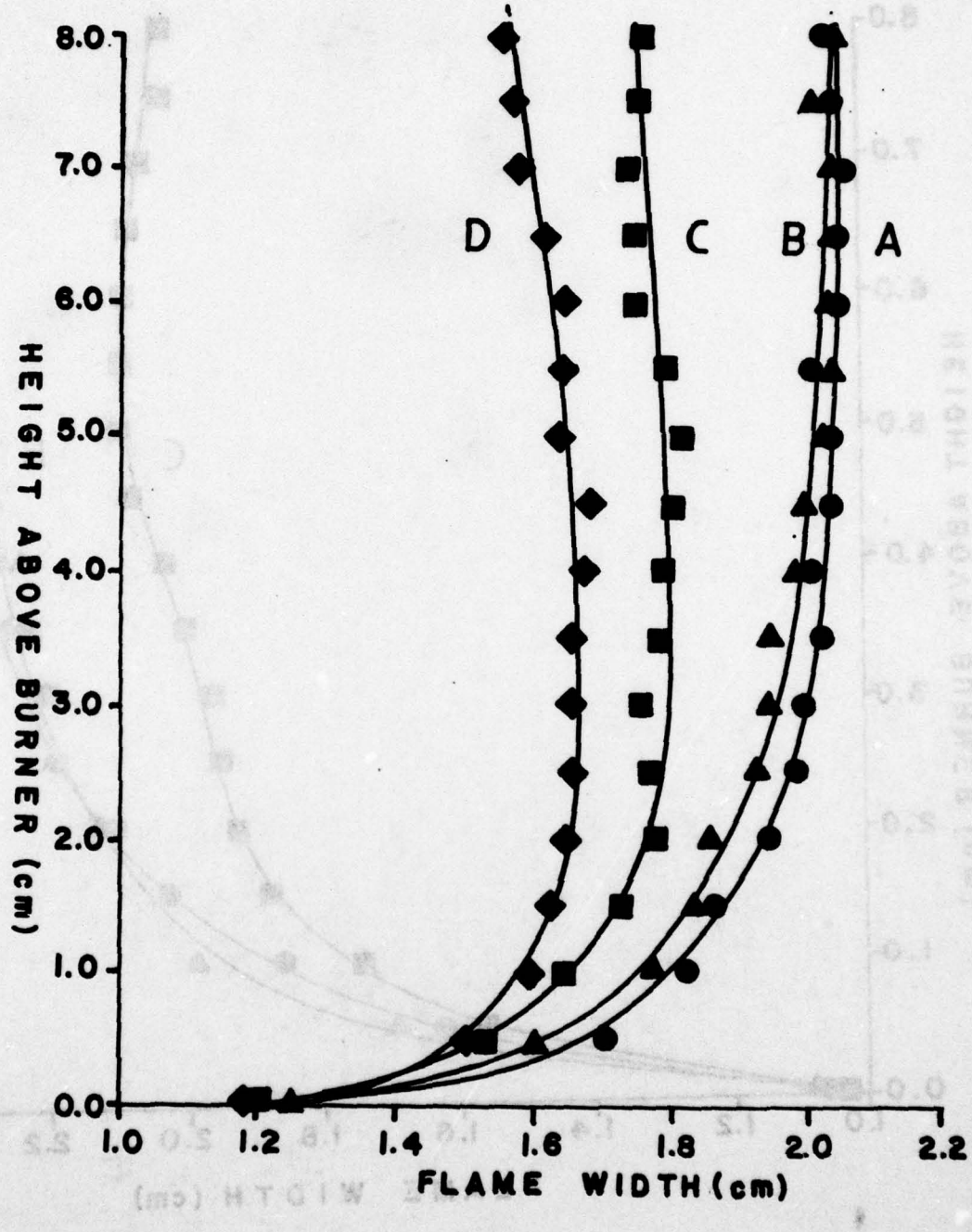
8.0
7.0
6.0
5.0
4.0
3.0
2.0
1.0
0.0
HEIGHT ABOVE BURNER (cm)
1.0
1.2
1.4
1.6
1.8
2.0
2.2
FLAME WIDTH (cm)
D
C
B
A

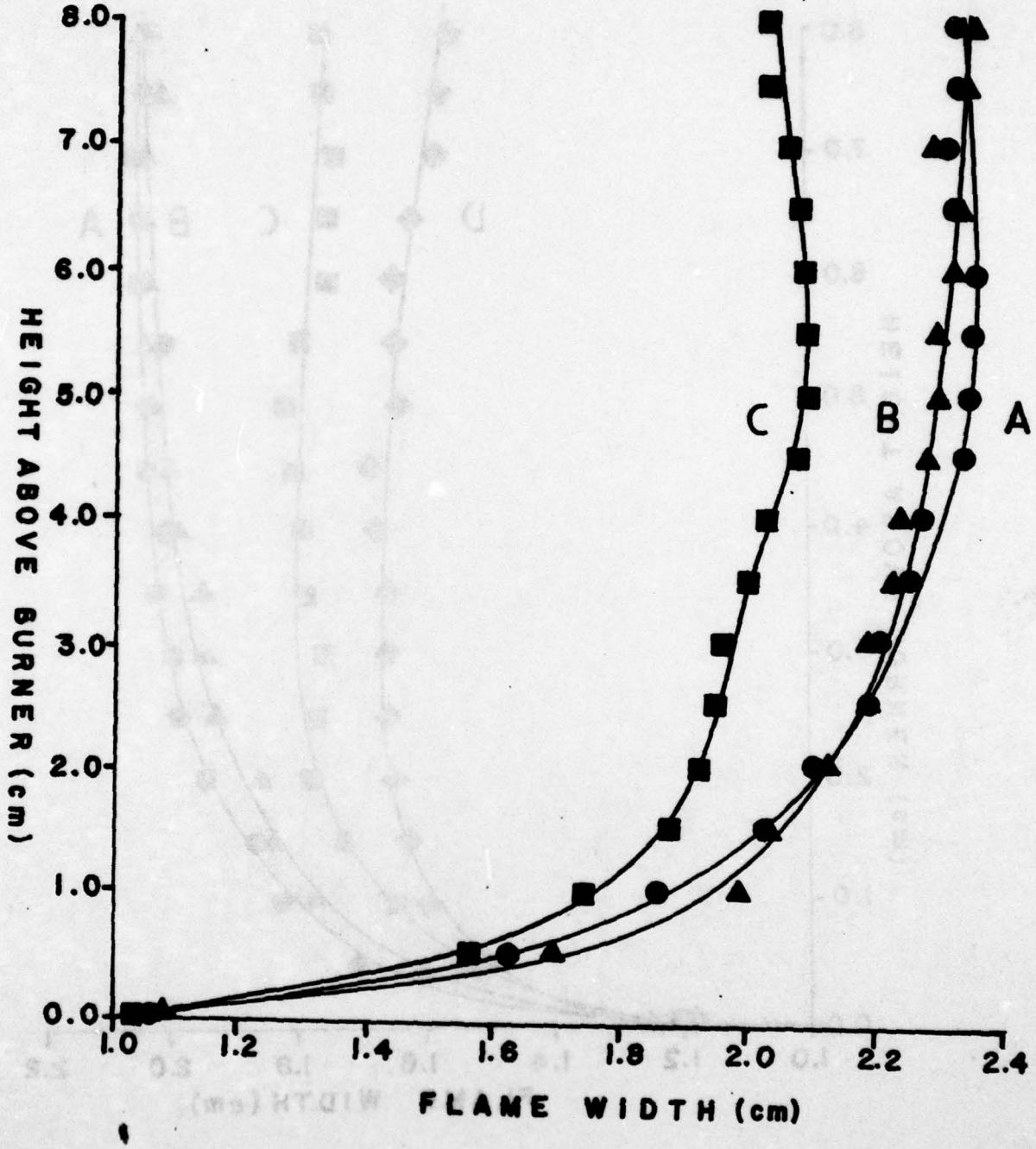
8.0
7.0
6.0
5.0
4.0
3.0
2.0
1.0
0.0
HEIGHT ABOVE BURNER (cm)
1.0
1.2
1.4
1.6
1.8
2.0
2.2
2.4
FLAME WIDTH (cm)
C
B
A

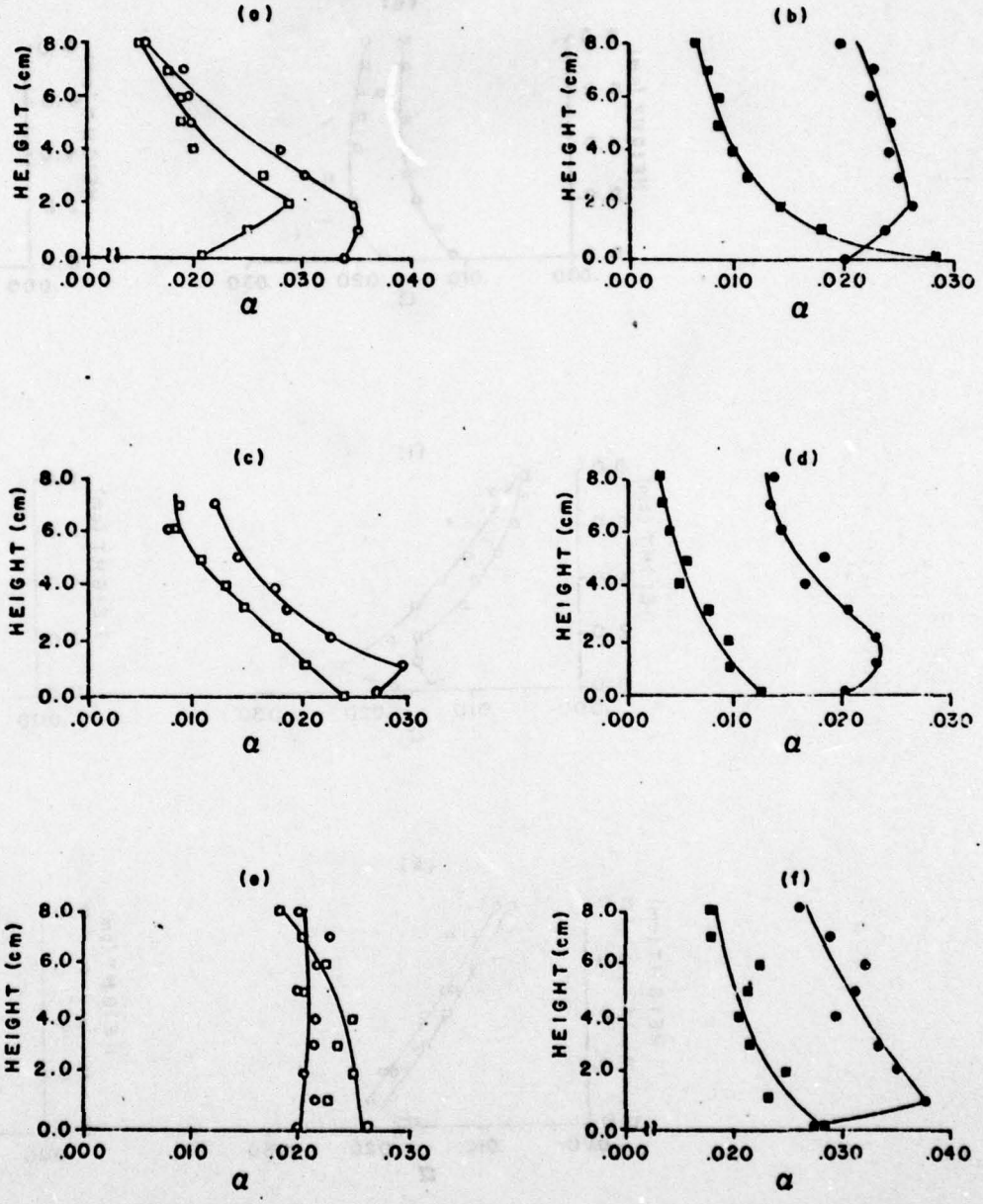
(a)
(b)
(c)
(d)
(e)
(f)
HEIGHT (cm)
8.0
6.0
4.0
2.0
0.0
.000
.010
.020
.030
.040
α

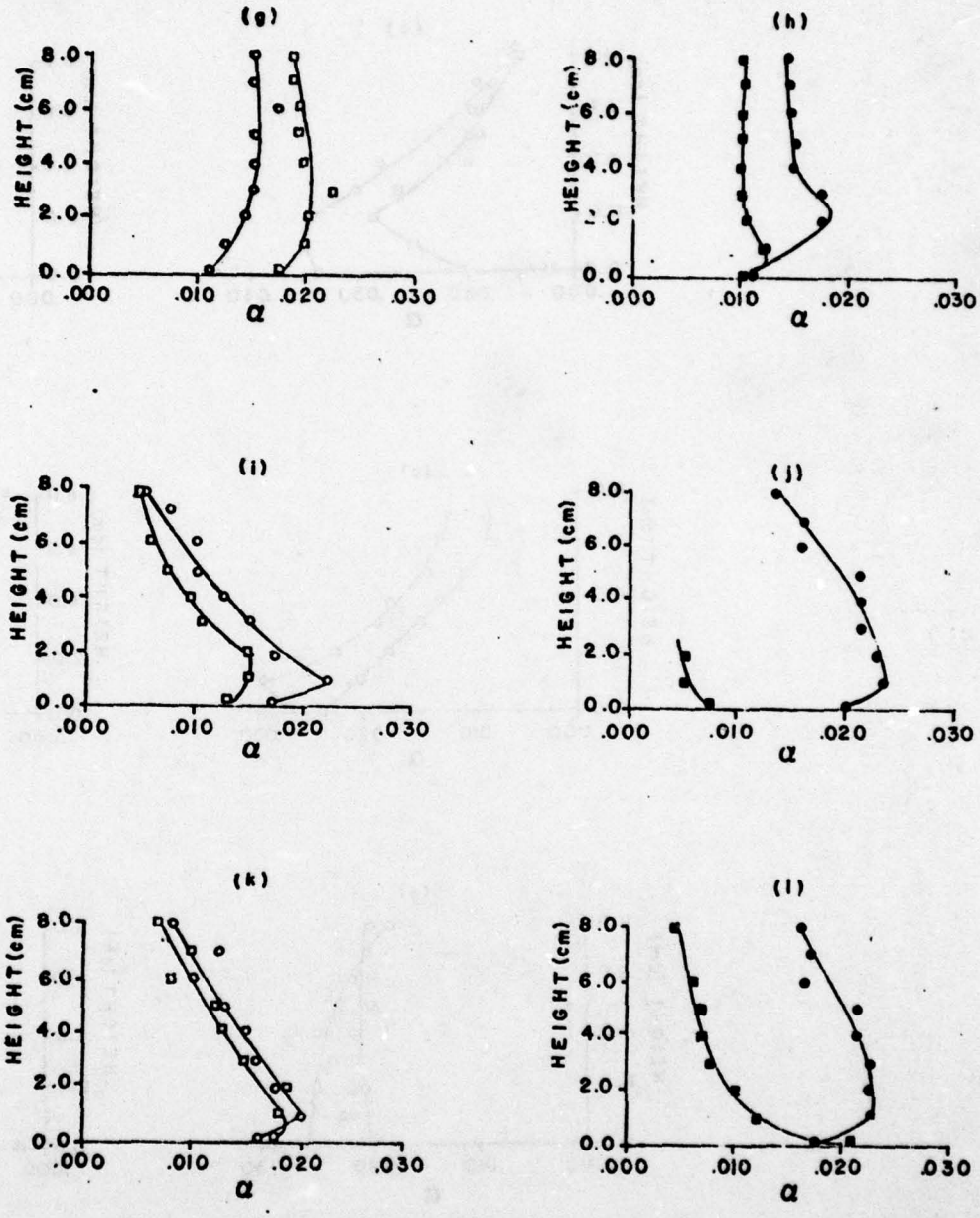
(g)
(h)
(i)
(j)
(k)
(l)
HEIGHT (cm)
8.0
6.0
4.0
2.0
0.0
.000
.010
.020
.030
α

472:GAN:716:tam
78u472-608

TECHNICAL REPORT DISTRIBUTION LIST, GEN

	No. Copies
Office of Naval Research 800 North Quincy Street Arlington, Virginia 22217 Attn: Code 472	2
ONR Branch Office 536 S. Clark Street Chicago, Illinois 60605 Attn: Dr. George Sandoz	1
ONR Branch Office 715 Broadway New York, New York 10003 Attn: Scientific Dept.	1
ONR Branch Office 1030 East Green Street Pasadena, California 91106 Attn: Dr. R. J. Marcus	1
ONR Area Office One Hallidie Plaza, Suite 601 San Francisco, California 94102 Attn: Dr. P. A. Miller	1
ONR Branch Office Building 114, Section D 666 Summer Street Boston, Massachusetts 02210 Attn: Dr. L. H. Peebles	1
Director, Naval Research Laboratory Washington, D.C. 20390 Attn: Code 6100	1
The Assistant Secretary of the Navy (R,E&S) Department of the Navy Room 4E736, Pentagon Washington, D.C. 20350	1
Commander, Naval Air Systems Command Department of the Navy Washington, D.C. 20360 Attn: Code 310C (H. Rosenwasser)	1
Defense Documentation Center Building 5, Cameron Station Alexandria, Virginia 22314	12
U.S. Army Research Office P.O. Box 1211 Research Triangle Park, N.C. 27709 Attn: CRD-AA-IP	1
Naval Ocean Systems Center San Diego, California 92152 Attn: Mr. Joe McCartney	1
Naval Weapons Center China Lake, California 93555 Attn: Dr. A. B. Amster Chemistry Division	1
Naval Civil Engineering Laboratory Port Hueneme, California 93401 Attn: Dr. R. W. Drisko	1
Professor K. E. Woehler Department of Physics & Chemistry Naval Postgraduate School Monterey, California 93940	1
Dr. A. L. Slafkosky Scientific Advisor Commandant of the Marine Corps (Code RD-1) Washington, D.C. 20380	1
Office of Naval Research 800 N. Quincy Street Arlington, Virginia 22217 Attn: Dr. Richard S. Miller	1
Naval Ship Research and Development Center Annapolis, Maryland 21401 Attn: Dr. G. Bosmajian Applied Chemistry Division	1
Naval Ocean Systems Center San Diego, California 91232 Attn: Dr. S. Yamamoto, Marine Sciences Division	1

Encl 1

TECHNICAL REPORT DISTRIBUTION LIST, 051C

	No. Copies
Dr. M. B. Denton University of Arizona Department of Chemistry Tucson, Arizona 85721	1
Dr. R. A. Osteryoung Colorado State University Department of Chemistry Fort Collins, Colorado 80521	1
Dr. B. R. Kowalski University of Washington Department of Chemistry Seattle, Washington 98105	1
Dr. S. P. Perone Purdue University Department of Chemistry Lafayette, Indiana 47907	1
Dr. D. L. Venezky Naval Research Laboratory Code 6130 Washington, D.C. 20375	1
Dr. H. Freiser University of Arizona Department of Chemistry Tucson, Arizona 85721	
Dr. Fred Saalfeld Naval Research Laboratory Code 6110 Washington, D.C. 20375	1
Dr. H. Chernoff Massachusetts Institute of Technology Department of Mathematics Cambridge, Massachusetts 02139	1
Dr. K. Wilson University of California, San Diego Department of Chemistry La Jolla, California 92037	1
Dr. A. Zirino Naval Undersea Center San Diego, California 92132	1
Dr. John Duffin United States Naval Postgraduate School Monterey, California 93940	1
Dr. G. M. Hieftje Department of Chemistry Indiana University Bloomington, Indiana 47401	1
Dr. Victor L. Rehn Naval Weapons Center Code 3813 China Lake, California 93555	1
Dr. Christie G. Enke Michigan State University Department of Chemistry East Lansing, Michigan 48824	1
Dr. Kent Eisentraut, MBT Air Force Materials Laboratory Wright-Patterson AFB, Ohio 45433	1
Walter G. Cox, Code 3632 Naval Underwater Systems Center Building 148 Newport, Rhode Island 02840	1